Analysis of Induction Motor with broken rotor bars Using Finite Element Method

Salah Eddine Zouzou, Samia Khelif, Noura Halem and M. Sahraoui
Electrical Engineering Laboratory of Biskra,
Biskra , Algeria,
E-Mail : zouzou_s@hotmail.com

Abstract - **The paper presents the use of the two-dimensional finite element method for modelling the three-phase squirrel-cage induction motor by using circuit-field coupled method. In order to analyze the machine performances, the voltage source is considered. The flux 2D magnetic analysis software is used for calculating the magnetic field of an induction motor having a cage fault. The simulation results of transient and steady state are given, which verifies the reliability of this method. The experimental results prove that the proposed approach constitutes a useful tool for the study and diagnostics of induction motors.**

Keywords - Induction motor, finite element, broken rotor bars, time stepping finite element (TSFE), diagnosis, faults.

I. INTRODUCTION

Rotor faults of induction machines yield asymmetrical operation of this one, causing unbalanced currents, torque pulsation, increased losses and decreased average torque. The need for detection of rotor faults at an earlier stage, so that maintenance can be scheduled, has pushed the development of monitoring methods with increasing sensitivity and noise protection. For that, a model closer to reality considering faults conditions must be established. An analytical analysis method based on the rotating field theory and coupled circuit was used [1]. In works, where the machine inductances are calculated and the machine performance is studied under faulty conditions, the Winding Function Approach (WFA), is used, where several assumptions and approximations of the actual machine layout are made, like the effects of stator teeth and slots, which are omitted in the calculations[2].

The modelling with finite element method represents a high fidelity electromagnetic behaviour. Which leads to more precise results than other models, as the actual geometry and winding layout of the machine are used. The consideration of the behaviour of the local electromagnetic induction machine provides a more accurate modelling. The numerical solution of Maxwell's equations governing the behaviour of electromagnetic fields and the consideration of the equations representing the electrical supply circuit of the machine reduces the simplifications made in the classical models. In analysis of induction motors, the input current, not the voltage, is usually used. The voltage source which is mainly discussed in this paper is more suitable than current source. The external circuit that represents the electrical sources and circuit components are coupled to the FEM. Only the terminal voltages applied to the motor are required as known input quantities, and the total terminal currents are the unknowns to be evaluated.

The use of time-stepping finite elements is the most precise way, up to date, for modelling the coupled field-circuits and motion of induction motors, accounting for both saturation, time and space harmonics. Indeed, the modelling of rotor mechanical motion and stator field source variation simultaneously allows coupling the instantaneous fields of stator and rotor [3]-[6].

This paper presents the transient state modeling of cage induction motors using the coupled electric circuit with 2D finite element electromagnetic field analysis. The flux 2D magnetic analysis software is used for calculating the magnetic field of an induction motor for the normal rotor, and for broken bars.

II. FINITE ELEMENT MODEL

Generally, the electric machine and apparatus are excited by connecting the external constant power source. Thus, it is necessary that the characteristics will be calculated under the constant terminal voltage. In this paper, the three-phase induction motor is analyzed by finite element method taking into account the terminal voltage. All the stator and rotor slots are represented in the circuit domain by defining real constants to conductor area in the FE domain. The motor is excited to its rated voltage and frequency using a three-phase voltage source.

The ratings of the machine are presented in Table I.

TABLE I. CHARACTERISTICS OF THE MACHINE

Variable	Value
Rated Power	1.1 kW
Rated Voltage	230 V
Frequency	50 Hz
Rated Speed	1425 rpm
Number of stator slots	36
Number of rotor bars	28

This work was supported by the DGRST, with PNR (ALGERIA)

Fig. 1 shows a detail of the mesh used for simulation. The magnetic circuit of squirrel cage and the geometry are very close to the real machine.

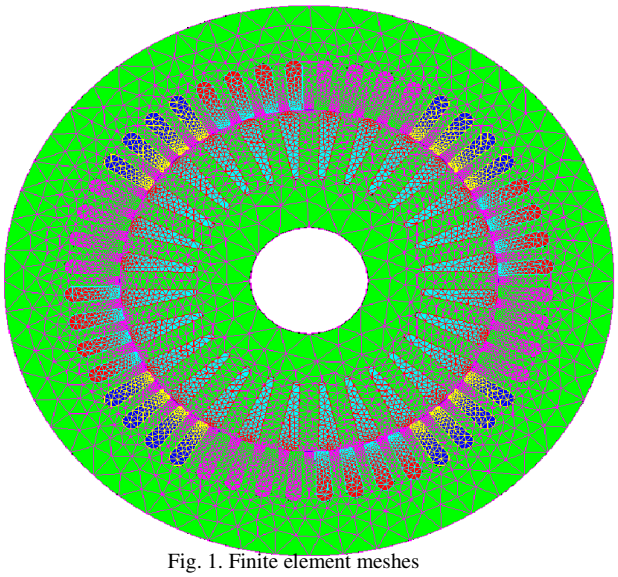

Fig. 1. Finite element meshes

III. SIMULATION RESULTS

In this paper, the induction motor is simulated under rated conditions. Fig. 2 shows the magnetic field distribution at steady state for healthy rotor. When the slip is small, the eddy current in the secondary conductor is small either. Therefore, the flux passes through the inside of rotor because of small effect of the field caused by eddy current. But above this, the results show that flux distribution is symmetrical in each pole.

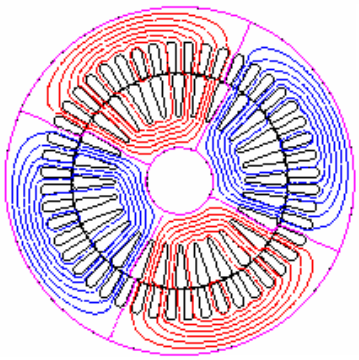

Fig. 2. Magnetic field distribution.

Fig. 3 shows the magnetic flux distribution for healthy rotor and with one broken bar at the transient state. When the slip is large, the eddy current shows a large value. This high value of slip is necessary to illustrate the effects of the broken bars on the field. The concentration of magnetic flux is observed around the broken bar and creates asymmetric magnetic flux distribution [7]-[9].

One can notice that the region around the broken bar of the rotor has a higher degree of saturation in comparison to the same region with no broken bars [10]. This is due to the fact that in the broken bar region there is no localized conductor demagnetization effect since these bars carry no currents [11].

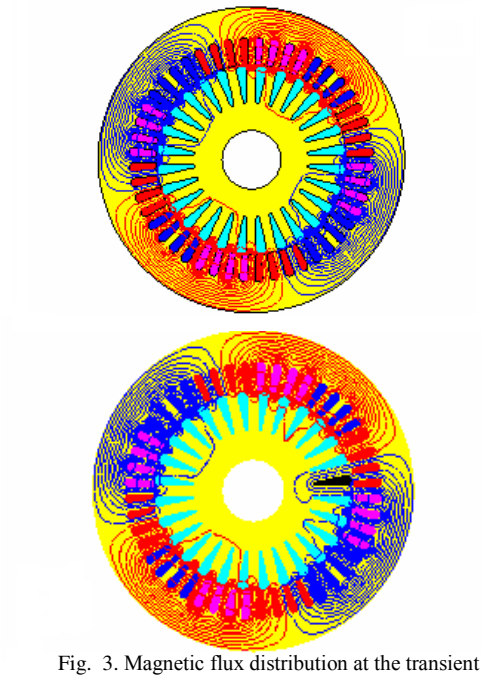

Fig. 3. Magnetic flux distribution at the transient state
Top: Healthy rotor, Bottom: One broken bar

Fig. 4 shows the waveform of the air gap flux density along a circular contour in the air-gap. The flux densities have a symmetrical distribution in healthy state. The perturbation in the magnetic field produced by 5 broken bars results in a non-symmetrical field [12].

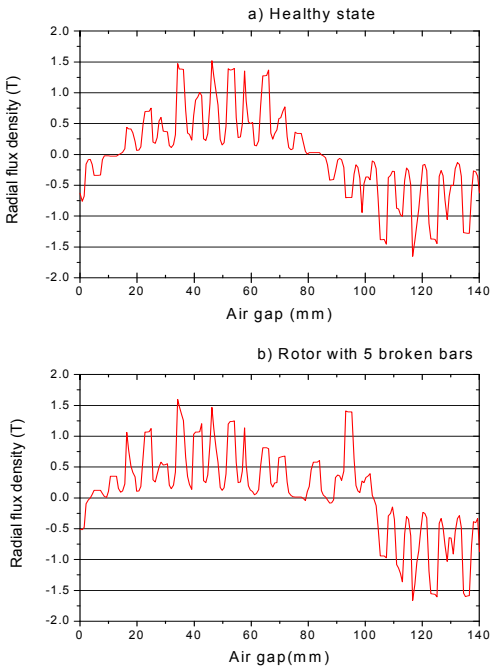

Fig. 4. Waveform of the Air gap flux density

Once the magnetic field is determined by the time-stepping finite-element method, the magnetic torque is calculated using

the Maxwell stress tensor. The mechanical equation determines a new angular and radial position of the rotor. The time increment used for the numeric integration was 0.0001.
The evolution of the stator current, speed and torque transients during the first second after the connection, for the case of healthy rotor are shown, respectively in fig. 5, 6 and 7.

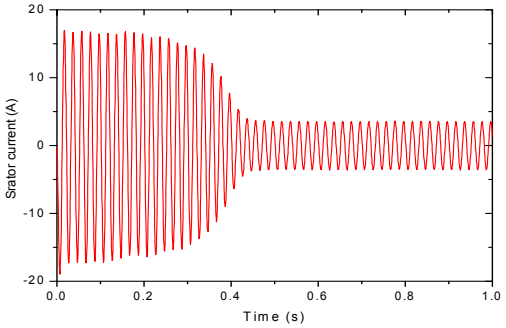

Fig.5. Stator current

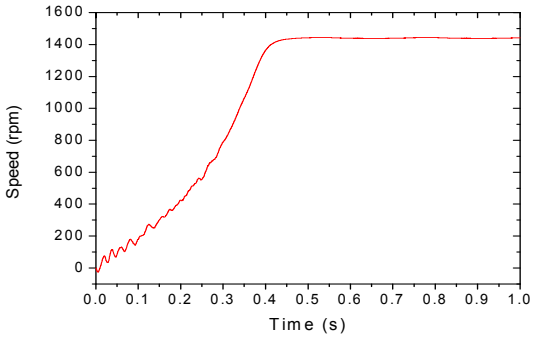

Fig.6. Speed

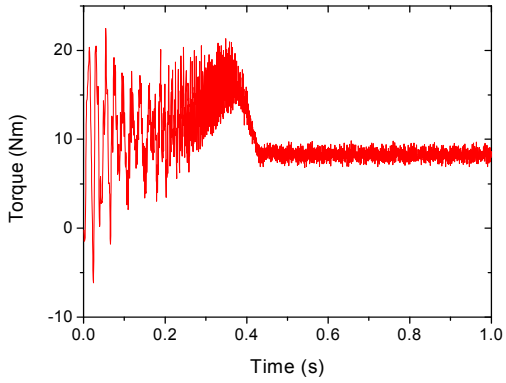

Fig.7. Electromagnetic torque

IV. EXPERIMENTAL RESULTS

In order to validate the simulation results, a special test model was used. It is a 1.1kW 220/380V 50Hz four pole induction motor whose stator windings were modified in order to have accessible several tapping. That can be used to introduce inter-turn short circuits with different number of turns. This test bench is available at the LAII in Poitiers, France.

Fig. 8 shows the stator current at steady state for loaded machine of simulation analysis and experimental results. We can notice a good agreement between the results.

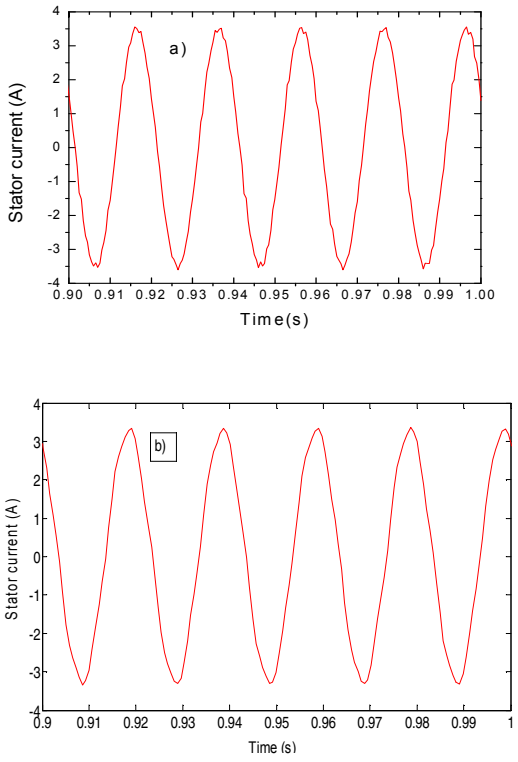

Fig.8. Stator Current at steady state
a) Computed
b) Measured

V. SPECTRUM ANALYSIS OF STATOR CURRENT

An induction machine rotor asymmetry introduced by broken bars produces spectrum lines of stator current at frequencies:

$$f_{bb1} = f_s(1 \pm 2ks) \qquad (1)$$

Where f_s is the electrical supply frequency, s is the slip, $k = 1, 2, 3, \ldots,$ respectively.

In Fig. 9, the spectra of the simulated stator current with healthy rotor and with one broken bars are presented. In case of broken rotor bar, the rotor is electrically asymmetric and the backward rotating field is created. The current spectrum reveals sidebands expected around the supply frequency given by (1) [13]-[14].

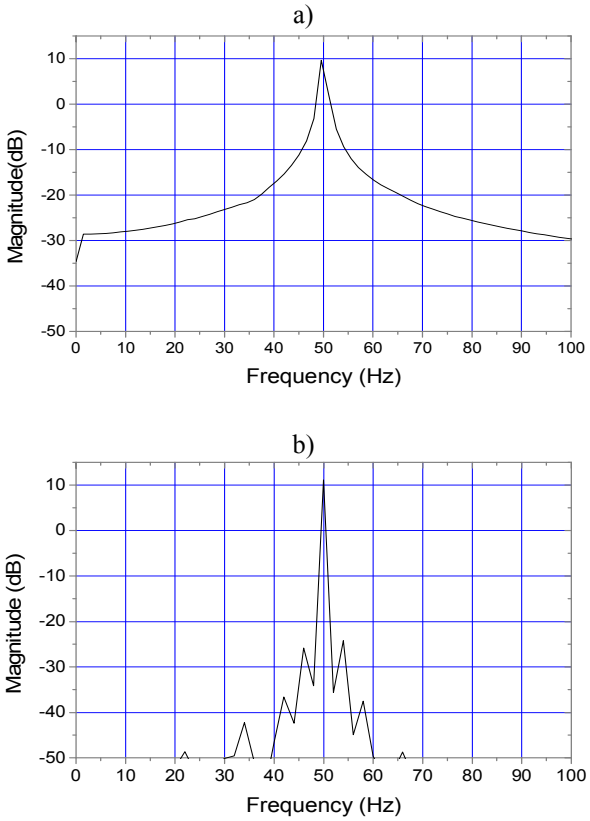

Fig. 9. Simulated current spectrum
a) Healthy rotor
b) Rotor with 1 broken bar

In order to have a better understanding of rotor broken bar, it may be necessary to examine the higher frequency components of the frequency spectra. When we took into account the space harmonics, additional frequency appear at frequencies given by:

$$f_{bb2} = f_s \left\{ \frac{k}{p}(1-s) \pm s \right\} \qquad (2)$$

Where, p is the number of pole pairs and k/p = 1, 3, 5, 7….

The spectra of the stator current of a loaded machine when it runs in healthy conditions are shown in Fig. 10. It is obvious that besides the supply frequency component, higher frequency components exist around the principal slot Harmonics as was predicted. Some frequency components (250Hz, 350Hz, etc.) exist which are a result of the saturation of magnetic material. Due to the configuration of three phase windings, harmonic orders that exist are: k/p = 1, 5, 7, 11…

In this simulation, magnetic saturation patterns cause the 3 rd harmonic and it's multiple to appear as non-zero components in the spectra of the phase currents. The spectra of the stator current of a loaded machine when it runs in faulty conditions are shown in Fig. 11. The stator current frequency described by (1) and (2) can be detected over the observation bandwidth between 0 Hz and 1000 Hz.

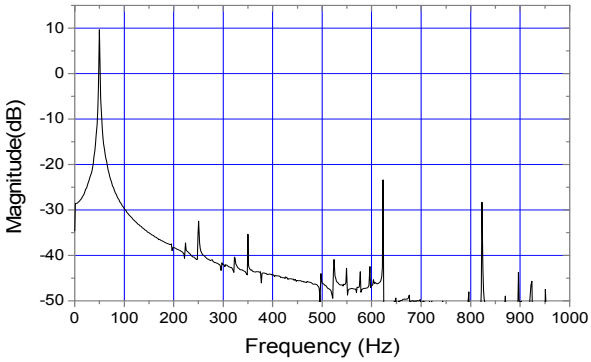

Fig.10. Simulated current spectrum

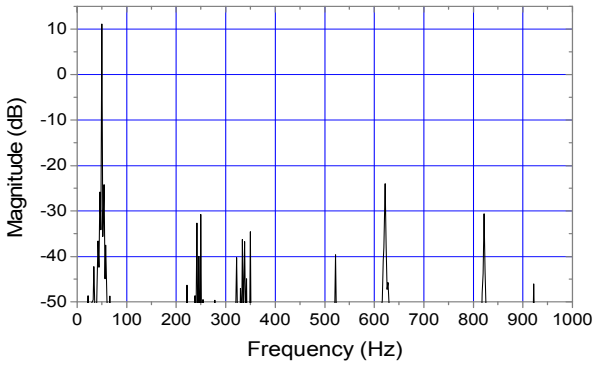

Fig.11. Simulated current spectrum with one broken bar

The spectrum of Fig. 12 shows the measured current waveform spectra with healthy rotor and with one broken bar. The current spectrum reveals sidebands expected around the supply frequency. Even for a motor in a healthy state, there are always frequency components but of low amplitudes, this is due to the natural asymmetry of the motor, and on the other hand from the power supply (distortion in the power supply voltage waveform). As can be clearly seen through Fig. 12, the occurrence of one broken rotor bar increases significantly the magnitudes of several sidebands around the fundamental.

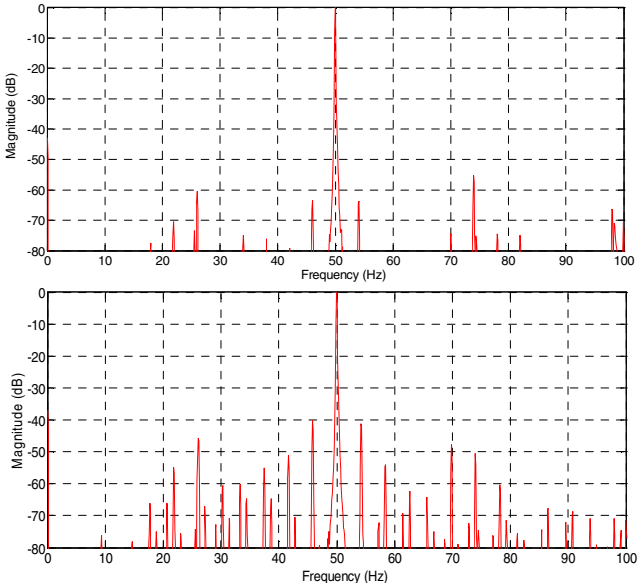

Fig.12. Measured Current spectrum
Top: Healthy rotor, Bottom: one broken bar

The spectrum of Fig. 13 shows the measured current waveform spectra with healthy rotor. We notice the presence of the slot harmonics in addition to the harmonics due to saturation. The lower rotor slot harmonic is visible at 620 Hz. As envisaged during simulation, we show the presence of the harmonics components of high frequencies. In order to avoid any misinterpretation, all spectral components having magnitudes less than -70 dB are assumed as noise.

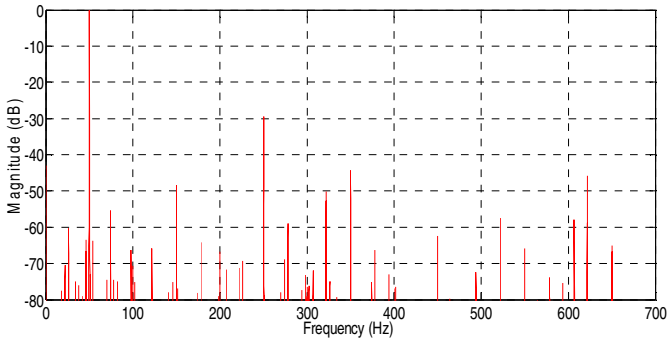

Fig.13. Measured current spectrum

Furthermore, the Fig. 14 shows, clearly, considerable changes in magnitude for the sidebands around the 3rd, 5th and 7th current time harmonics, for a motor with one broken bar.

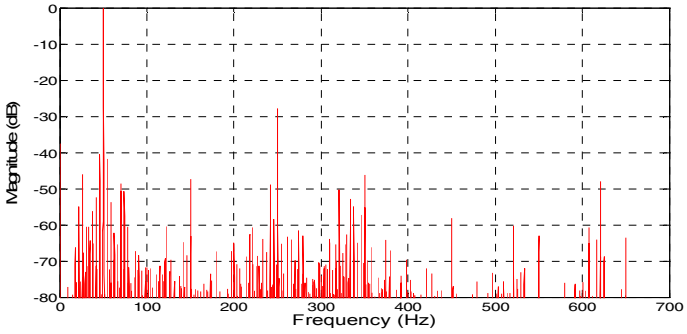

Fig.14. Measured current spectrum with one broken bar

VI. CONCLUSION

This paper presents the circuit coupled finite element method used to modeling the Three-Phase Squirrel Cage Induction Motor. For this purpose, the time-stepping finite element method (TSFE) was proposed. The determination of magnetic flux density waveform, magnetic flux distribution was obtained. The perturbation in the air-gap magnetic field produced by broken bars results in a non-symetrical field. The stator current waveform obtained with simulation was in good agreement with the experimental results. The simulation waveforms of speed and torque transients of induction motor during start-up confirm the known experimental results. As envisaged during simulation, the presence of harmonics in current spectra at low and high frequency confirm the experimental results, proving that the proposed approach constitutes a useful tool for the study and diagnostics of induction motors. It will be mentioned that this approach is limited only to the evaluation of the component frequencies induced by the broken bars fault.

ACKNOWLEDGMENTS

The authors would like to thank Professor Champenois at the LAII laboratory, Poitiers, France, for his help.

REFERENCES

[1] A. Ghoggal, M. Sahraoui and S. E. Zouzou, " Analytical and experimental study of a squirrel cage induction motors with rotor bar faults," *Advances in Modelling, Measurement and Control,A : General Physics and Electrical Applications*, AMSE, vol. 81, no. 2, pp. 43-60, 2008.

[2] S. E. Zouzou, A. Ghoggal, A. Aboubou, M. Sahraoui, and H. Razik, "Modelling of induction machines with skewed rotor slots dedicated to rotor faults," presented at the IEEE International Symposium on Diagnostics for Electric Machines, Power Electronics and Drives, Vienna, Austria, 7-9 Sep. 2005.

[3] Y. Ouazir, N. Takorabet, R. Ibtiouen, and M. Benhaddadi, "Time-stepping FE analysis of cage induction motor with air-gap interface coupling taking Into account phase-belt harmonics," *IEEE Trans. Magn*, vol. 45, pp.1384-1387, Mar. 2009.

[4] J. Faiz, B. M. Ebrahimi, and M. B. B. Sharifian, "Time stepping finite element analysis of broken bars fault in a three-phase squirrel-cage induction motor," Progress In Electromagnetics Research, vol. 68, pp. 53-70, 2007.

[5] J. F. Bangura, N. A. Demerdash, "Diagnosis and characterization of effects of broken bars and connectors in squirrel-cage induction motor by time-stepping coupled FE state space modeling approach," *IEEE Trans. Energy Convers.*, vol. 14, pp. 1167–1176, Apr. 1999.

[6] X. Ying, "Characteristic performance analysis of squirrel cage induction motor with broken bars," *IEEE Trans. Magn*, vol. 45, pp. 759-766, Feb. 2009.

[7] R. Fiser, S. Ferkolj, "Application of a finite element method to predict damaged induction motor performance," *IEEE Trans. Magn,* vol. 37, Part 1, pp.3635-3639, September 2000.

[8] G. H. Jang, S. J. Park, "Simulation of the electromechanical faults in a single-phase squirrel cage induction motor," *IEEE Trans. Magn*, vol. 39, pp.2618-2620, Sep. 2003.

[9] C. J. Aileen, S. Nagarajan and S. R. Reddy, "Detection of broken bars in three phase squirrel cage induction motor using finite element method," presented at the International Conference on Emerging Trends in Electrical and Computer Technology (ICETECT), Nagercoil, India, 23-24 Mar. 2011.

[10] J. Sprooten, J. C. Maun, "Influence of saturation level on the effect of broken bars in induction motors using fundamental electromagnetic laws and finite element simulations," *IEEE Trans. Energy Convers.*, vol. 24, pp. 557-564, Sep. 2009.

[11] L. Weili, X. Ying, S. Jiafeng, L. Yingli, "Finite-element analysis of field distribution and characteristic performance of squirrel-cage induction motor with broken bars," *IEEE Trans. Magn.*, vol. 43, pp. 1537 – 1540, Apr. 2007.

[12] K. J. Hammadi, D. Ishak, and W. Salah, "Rotor fault diagnosis based on current signatures in squirrel-cage induction motor,"presented at the International Conference on Electronic Devices, Systems and Applications (ICEDSA), Kuala Lumpur, Malaysia, pp. 200-205, 11-13 Apr. 2010.

[13] M. Riera-Guasp, M. F. Cabanas, J. A. Antonino-Daviu, M. Pineda-Sanchez, and C. H. R. Garcia, "Influence of nonconsecutive bar breakages in motor current signature analysis for the diagnosis of rotor faults in induction motors," *IEEE Trans. Energy Convers.*, vol. 25, pp.80-89, March 2010.

[14] J. Faiz, B. M. Ebrahimi, "Locating rotor broken bars in induction motors using finite element method," *Energy Conversion and Management*, vol. 50, pp. 125-131, Jan. 2009.